Paper No. T6-2.1, pp. 1-5

15th INTERNATIONAL SYMPOSIUM on POWER ELECTRONICS - Ee 2009
XV Međunarodni simpozijum Energetska elektronika – Ee 2009
NOVI SAD, REPUBLIC OF SERBIA, October 28th - 30th, 2009

ANALYSIS OF HARMONIC LOSSES IN MULTI-PHASE DRIVES

Dražen Dujić, Martin Jones*, Emil Levi*
ABB Corporate Research, Baden-Dättwil, Switzerland
*Liverpool John Moores University, School of Engineering, Liverpool, UK

Abstract: *Multi-phase variable speed drives, supplied from two-level voltage source inverters (VSIs), are currently considered for a number of industrial applications. While various multi-phase PWM schemes had been developed, only a limited progress has been made with regard to the impact of these schemes on harmonic losses (current ripple). This paper presents a general analytical analysis and comparison of harmonic losses of two basic continuous PWM (CPWM) schemes aimed at sinusoidal output voltage generation with multi-phase VSIs. Two different methods are presented, based on the use of the space vector theory and the concept of multiple polygon connections, respectively. As a result, harmonic distortion factors (HDFs) of sinusoidal PWM (SPWM) and harmonic injection PWM (HIPWM) are determined and compared for various phase numbers. Theoretical findings are verified experimentally using a five-phase induction motor drive.*

Key Words: ***Multi-phase Drives, PWM, Harmonic Losses, Harmonic Distortion Factor***

1. INTRODUCTION

Analytical tools, developed for the analysis of harmonic losses (output current ripple) of three-phase systems, are based either on the application of the space vector theory [1-2] or on the analysis in the original domain [3-6]. In the latter case the output current ripple rms is analysed by considering delta connection of machine windings [3-6]. Regardless of the approach selected, harmonic distortion factors (HDFs) are obtained for each PWM scheme, which allows a simple graphical comparison. As is well known, in three-phase drives injection of the third harmonic improves the output current ripple rms, while simultaneously increasing the dc bus utilization over the level offered by the SPWM [1-6]. While a further reduction of the harmonic losses is possible by means of discontinuous PWM schemes, such multi-phase PWM algorithms are beyond the scope of this paper. The analysis is restricted to CPWM multi-phase techniques of SPWM and HIPWM type [7].

While windings of a three-phase machine can be connected either in star or delta, windings of multi-phase machines can be connected in star or in a certain number of polygons [8]. Thus, like in a three-phase system, either space vector approach [9] or the analysis based on the polygon connections [10-11] can be used for the analysis of harmonic losses of multi-phase drives. While final results (HDFs) are the same, there are some differences during application of each of the approaches.

The analysis presented in this paper is of a completely general nature, so that the determined HDFs fully include the existing knowledge [1-6] for both SPWM and HIPWM and provide a further generalization of HDFs for any *n*-phase system with an odd number of phases and a single isolated neutral point.

On the basis of the developed theory it is shown that the harmonic losses cannot be reduced in multi-phase systems by means of the zero-sequence harmonic injection, in contrast to the three-phase case. Theoretical findings are validated through experimental investigation on a five-phase drive.

2. SQUARE WAVE MODE OF OPERATION

It is initially interesting to explore harmonic content of an *n*-phase two-level VSI operating in square-wave mode (2*n*-step mode). Per-phase weighted THD (WTHD) for such an inverter is given with (*m* represents the harmonic order) [6]:

$$WTHD_{sqw-n} = \sqrt{\sum_{m=3,5,7,\ldots}^{\infty} \frac{1}{m^4}} \tag{1}$$

For a single-phase inverter this can be calculated as:

$$WTHD_{sqw-1} = \sqrt{\frac{\pi^4}{96} - 1} = 0.1212 \tag{2}$$

For all the other odd *n*-phase two-level VSIs, WTHD can be determined in a general form as:

$$WTHD_{sqw-n} = \sqrt{\frac{\pi^4}{96}\left(1 - \frac{1}{n^4}\right) - 1} \tag{3}$$

Result of plotting (3), for the number of phases up to fifteen, are shown in Fig. 1. It can be observed that WTHD of the three-phase VSI is the lowest and that, as the number of phases increases, WTHD initially increases as well, but then saturates and becomes practically independent of the phase number. For $n \to \infty$, WTHD becomes equal to WTHD of the single phase inverter. Although in PWM operation low-order harmonics present in (1)-(3) do not exist, Fig. 1 gives some indication of the trend in the harmonic losses that can be expected as the number of phases of a system increases.

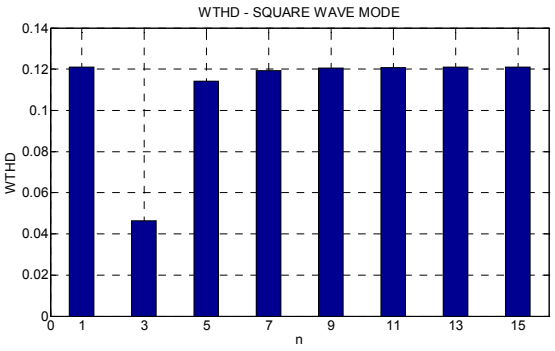

Fig. 1. *Per-phase WTHD in the square-wave mode of operation of an n-phase VSI.*

3. BASIC PWM METHODS FOR MULTI-PHASE INVERTERS

Two basic CPWM schemes, aimed at generation of sinusoidal output voltages, are considered in order to evaluate output current ripple rms in multi-phase drives. In terms of the carrier-based PWM approach, the modulating signals are defined, in general, as:

$$v_i = v_i^* + v_{zs} \tag{4}$$

where v_i^* are the fundamental sinusoidal signals (displaced in time by $2\pi/n$) while v_{zs} is the zero-sequence signal. Different zero-sequence signals lead to different PWM schemes [6,12], and these are selected for SPWM and HIPWM, respectively, as:

$$v_{zs} = 0 \tag{5}$$

$$v_{zs} = bM\cos(n\vartheta) \tag{6}$$

Modulation index M is the ratio of the peak value of the fundamental phase voltage to one half of the dc bus voltage, $\vartheta = \omega t$, while parameter $b = -\sin(\pi/10)/n$ determines the relative amount of the n-th harmonic with respect to the fundamental and is selected in such a way that it maximizes dc bus utilization [13].

The generalized decoupling transformation in power-variant form is given for an n-phase system with ($\varphi = 2\pi/n$) [7]:

$$\underline{C}_n = \frac{2}{n}\begin{bmatrix} 1 & \cos(\varphi) & \cdots & \cos(n-1)\varphi \\ 0 & \sin(\varphi) & \cdots & \sin(n-1)\varphi \\ 1 & \cos(2\varphi) & \cdots & \cos 2(n-1)\varphi \\ 0 & \sin(2\varphi) & \cdots & \sin 2(n-1)\varphi \\ \vdots & \vdots & \vdots & \vdots \\ 1 & \cos(\frac{n-1}{2})\varphi & \cdots & \cos(\frac{n-1}{2})(n-1)\varphi \\ 0 & \sin(\frac{n-1}{2})\varphi & \cdots & \sin(\frac{n-1}{2})(n-1)\varphi \\ 1/2 & 1/2 & \cdots & 1/2 \end{bmatrix} \tag{7}$$

By combining successive pairs of rows into corresponding complex quantities, complex space vectors are obtained [7]. Transformation (7) decomposes an n-dimensional vector space into (n-1)/2 2-D and mutually orthogonal planes, which are defined with the first (n-1)/2 pairs of rows in (7), d_1-q_1, d_2-q_2, d_3-q_3, etc. The last row defines a single-dimensional zero-sequence sub-space that cannot be excited in the case of an isolated neutral point of a star-connected n-phase load.

Another important property of (7) is a clear mapping of harmonics of different order into different 2-D planes. For example, in a five-phase system, harmonics of the order $10k\pm1$ (k=0,1,2,…) are mapped into d_1-q_1 plane, and those of the order $10k\pm3$ into d_2-q_2 plane, in a seven-phase system harmonics of the order $14k\pm1$, $14k\pm3$ and $14k\pm5$ map into d_1-q_1, d_3-q_3 and d_2-q_2 plane, respectively, etc. The main idea behind the analysis reported here is to evaluate these harmonics around switching frequency multiples through the analysis of the output current ripple rms, for a selected PWM method.

If the space vector approach is used, the analysis has to be performed in all 2-D planes of an n-phase system in order to take into account all characteristic harmonics and obtain per-phase results. However, all of these harmonics are present in both phase voltages and line voltages. Unlike as in three-phase case, one can identify several ways to connect multi-phase machine's windings in polygons [8]. It is easy to establish that the number of different polygons of an n-phase machine (n = odd number) equals (n-1)/2, and is thus equal to the number of 2-D planes [8], as well as to the number of different line voltages of an n-phase system [14]. Thus polygon connections can be utilised as well, to evaluate harmonic content of line voltages.

Using a five-phase machine as an example, two possible polygon connections are shown in Fig. 2. In the first polygon connection (*P1*) phases of a load are connected between adjacent legs of the inverter (e.g., *A*-*B*), while non-adjacent legs are used in the second polygon connection (*P2*; e.g., *A*-*C*). Similarly, a seven-phase machine can be connected into three polygons, a nine-phase machine into four polygons, etc.

4. ANALYSIS OF OUTPUT CURRENT RIPPLE RMS

Foundation of the analysis is the same, regardless of the approach selected. Discrete nature of operation of the inverter introduces error voltage (difference between applied voltage and reference voltage) which causes the current to rise and fall around its average value (current ripple). To avoid the dependence on the inductance, notion of the harmonic flux can be used, defined as:

$$\Delta\bar{\lambda} = L\Delta\bar{i} = (\bar{v} - \bar{v}^*)\Delta t \tag{8}$$

where the term in the brackets represents the error voltage over the discrete time interval. Deviation of harmonic flux (8) has to be determined over each discrete interval within the switching period, and the number of the intervals is defined by the pattern of the switching sequence of the space vectors.

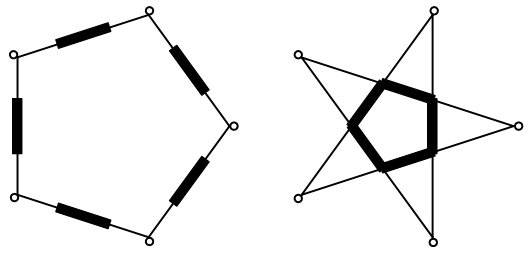

Fig. 2. *Polygon connections of five-phase machine windings: a) adjacent (P1), and b) non-adjacent (P2).*

4.1. Space vector approach

The second step involves an analysis of harmonic flux over the switching period (microscopic analysis). As a figure of merit, squared value of the harmonic flux over the switching period can be used, so that the following integral needs to be calculated:

$$\Delta\lambda^2{}_{RMS} = \frac{2}{T_s}\int_0^{T_s/2}\Delta\lambda^2 dt \tag{9}$$

Here $\Delta\lambda^2$ represents phase deviations of the harmonic flux, which are obtained by formulating the sum of the squares of the harmonic flux deviations in each phase and transforming them into two 2-D planes using the decoupling transformation (7). With this, all phases of the load are accounted for. Due to the symmetry, one half of the switching period is sufficient for the analysis.

As the third step of the analysis, squared harmonic flux (9) needs to be evaluated over the fundamental period (macroscopic analysis) in order to obtain a closed-form solution (HDF). Due to the symmetry, the first sector is again sufficient for the analysis and one needs to find the solution of the integral:

$$HDF = \Delta\lambda^2{}_{RMSF} = \frac{n}{\pi}\int_0^{\pi/n}\Delta\lambda^2{}_{RMS}\, d\vartheta \tag{10}$$

4.2. Polygon approach

Polygon connections simplify the analysis, since one phase of the load is effectively connected in between two inverter legs and exposed to the line voltage. Thus very general calculation can be performed, independently from the actual phase number of the system. For that, the second step (9) is the same as with space vector approach, but with different (lower) number of time intervals within the half of the switching period.

Final calculation again differs slightly, since line voltage is being evaluated, and is given as:

$$HDF = \Delta\lambda^2{}_{RMSF} = \frac{1}{\pi}\int_{\alpha-\pi}^{\alpha}\Delta\lambda^2{}_{RMS}\, d\vartheta \tag{11}$$

Here angle α is defined as $\alpha = p\,\pi/n$, while p takes the values from p = 1 to (n-1)/2 and corresponds to the polygon number. This generalization allows that, by varying the angle α, modulating signals for a variety of phase numbers and different polygons can be generated. Thus, it is enough to integrate over the positive half of the line voltage fundamental period which is always over the range ($\alpha - \pi \div \alpha$), regardless of the phase number or the polygon selected.

5. HARMONIC DISTORTION FACTORS OF FIVE-PHASE PWM SCHEMES

By applying the space vector approach to the case of five-phase SPWM and HIPWM, HDFs in both 2-D planes are obtained, where HDF in the d_2-q_2 plane ($10k$±3 harmonics) is the same for both considered PWM schemes and is given with:

$$HDF_5^{10k\pm3} = \frac{1}{3}\frac{32}{3\pi}K^3M^3 \tag{12}$$

On the other hand, each PWM scheme is with a unique solution in the d_1-q_1 plane ($10k$±1 harmonics):

$$HDF_{5-SPWM}^{10k\pm1} = \frac{1}{3}\left[\begin{array}{l}2(K^2+K_2^2)M^2 - \frac{32}{3\pi}(2K^3+K_2^3)M^3 \\ +\frac{3}{2}(K^2+K_2{}^2)M^4\end{array}\right]$$

$$HDF_{5-HIPWM}^{10k\pm1} = \frac{1}{3}\left[\begin{array}{l}2(K^2+K_2^2)M^2 - \frac{32}{3\pi}(2K^3+K_2^3)M^3 \\ +\frac{3}{2}(K^2+K_2{}^2)(1+2b^2)M^4\end{array}\right] \tag{13}$$

Trigonometric constant in (12) and (13) is defined as $K_p = \sin(\alpha)$ and, when p = 1, the sub-script is omitted. By adding (12) to (13) total HDFs for each PWM scheme are easily obtained. This is illustrated in Fig. 3a.

On the other hand, polygon approach produces the following generic HDFs for the two considered PWM schemes, valid for all polygons:

$$HDF_{n-SPWM}^{Pp} = \frac{1}{3}\left[2K_p^2M^2 - \frac{32}{3\pi}K_p^3M^3 + \frac{3}{2}K_p^2M^4\right] \tag{14}$$

$$HDF_{n-HIPWM}^{Pp} = \frac{1}{3}\left[\begin{array}{l}2K_p^2M^2 - \frac{32}{3\pi}K_p^3M^3 \\ +\frac{3}{2}K_p^2(1+2b^2)M^4\end{array}\right] \tag{15}$$

Since in a five-phase system, there are only two polygons to consider (p = 1 or 2), particular HDFs of each of the polygons can be easily derived from (14) and (15) (Fig. 3b), by introducing proper trigonometric constants where appropriate. Normalization factor used during plotting is the same as in [1-2] and equal to $\Delta\lambda_N = V_{dc}T_s/8$. From the results given in Fig. 3b it can be seen that HDFs for each polygon are completely different from HDFs for the planes obtained with space vector approach. However, the total HDF obtained by summation of the polygon HDFs is identical to the total HDF obtained by summation of HDFs in two planes.

It is easy to see that the HDF of the SPWM is with lower values than the one of the HIPWM, suggesting that injection of the n-th harmonic into an n-phase system (with n > 3) cannot improve the HDF. This can be further verified by checking the minimum of the (13) or (15) with b as a parameter.

6. RELATION BETWEEN SPACE VECTOR AND POLYGON APPROACH

In contrast to the application of the space vector theory, which inherently maps phase harmonics of the different order into different 2-D planes, analysis based on polygons gives the direct measure of line voltage harmonics. This does not represent a problem in a three-phase system, since the relation between phase voltage and line voltage harmonics is unique and governed by the $2K = \sqrt{3}$ scaling factor (as there is only a single line voltage).

However, in multi-phase systems (n > 3) the situation is significantly different [14]. In the general case, for harmonics of the order $2nk \pm l$ (l = 1,3,5,…; k = 0,1,2…) one has that scaling factors between various phase voltage harmonic magnitudes (V_l) and line voltage harmonic magnitudes are governed with:

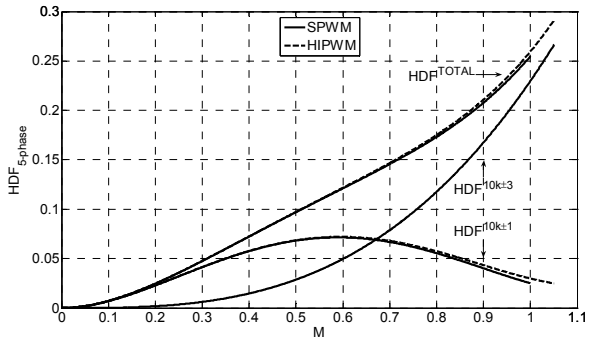

a)

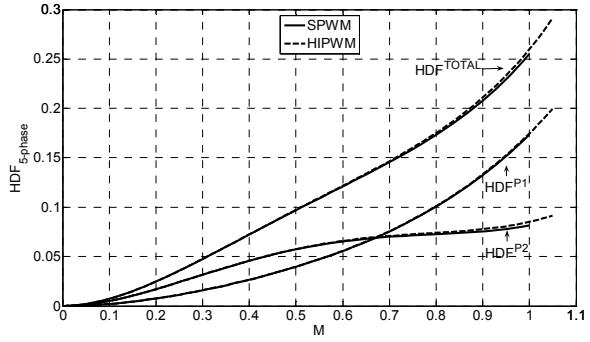

b)

Fig. 3. *HDFs of the five-phase PWM methods: a) total HDF and HDFs in the d_1-q_1 and d_2-q_2 plane, b) polygon HDFs and the total HDF.*

$$v_{ABl} = v_{al} - v_{bl} = -2K_l V_l \sin(\vartheta_c + \vartheta - l\alpha)$$
$$v_{ACl} = v_{al} - v_{cl} = -2K_{2l} V_l \sin(\vartheta_c + \vartheta - 2l\alpha) \quad (16)$$

where $\vartheta_c = \omega_c t$ and ω_c is the angular carrier frequency. Using again five-phase system as an example, phase voltage harmonics of the order $10k\pm1$ (d_1-q_1 plane) are related to $10k\pm1$ line voltage harmonics in polygons *P1* and *P2* with scaling factors $2K$ and $2K_2$, respectively. On the other hand, phase voltage harmonics of the order $10k\pm3$ (d_2-q_2 plane) are related to $10k\pm3$ line voltage harmonics in polygons *P1* and *P2* with (opposite) scaling factors $2K_2$ and $2K$.

Thus, HDF of any of the polygons on its own is not enough to obtain the correct per-phase HDF since phase harmonics of the different order are related with different scaling factors to the line voltage harmonic of the same order. Therefore, all polygon HDFs need to be considered together and one has, after considering relations among phase and line harmonics:

$$HDF_5^{P1} = (2K)^2 HDF_5^{10k\pm1} + (2K_2)^2 HDF_5^{10k\pm3}$$
$$HDF_5^{P2} = (2K_2)^2 HDF_5^{10k\pm1} + (2K)^2 HDF_5^{10k\pm3} \quad (17)$$

Since sum of $HDF_5^{10k\pm1}$ and $HDF_5^{10k\pm3}$ gives per-phase HDF, one has from (17):

$$HDF_5^{10k\pm1} + HDF_5^{10k\pm3} = \frac{HDF_5^{P1} + HDF_5^{P2}}{4(K^2 + K_2^2)} \quad (18)$$

Since for $n = 5$ the coefficient $4(K^2 + K_2^2) = 5$, per-phase HDF is actually 1/5 of the directly summed HDFs of two polygons. This represents total HDF of a five-phase system as already established. Further solving of (17) with known polygon HDFs yields HDFs in the d_1-q_1 and d_2-q_2 plane, as determined with (12) and (13). Similar considerations apply to other multi-phase systems.

Only final per-phase HDF and total HDF are generated and compared for the number of phases from three to nine (Fig. 4, SPWM only). It can be seen that the total SPWM HDF significantly increases as the number of phases increases (since it accounts for all phases, Fig. 4a). However, per-phase HDF in Fig. 4b shows the lowest value in a three-phase system, while in other multi-phase systems differences are rather small and gradually vanish with an increase in the phase number. This is in line with the expectations based on the analysis of the WTHD in $2n$–step mode (Fig. 1) in section 2.

7. EXPERIMENTAL RESULTS

Experimental results are collected from the star-connected five-phase induction motor drive. Both SPWM and HIPWM are implemented in a TMS320F2812 DSP-based control system. Switching frequency is set to 5 kHz and the motor operates in the open-loop *V/f* mode. Since FHIPWM yields 5.15% higher dc bus utilization [12-13], the *V/f* profile is adjusted in such a way that both PWM schemes operate with M=1 at 50 Hz. Only high frequency portion of the current spectrum is shown in Fig. 5 and it includes the harmonics of the first three carrier frequency sidebands.

High frequency spectrum plots appear very similar to each other and visible differences in magnitudes of various harmonic components are relatively small. Yet, it can be seen that the most pronounced differences are in the sideband harmonics around the first (5 kHz) and the third (15 kHz) carrier frequency harmonics. Magnitudes of these harmonics are with slightly lower values around 5 kHz and 15 kHz with SPWM than with HIPWM. In the 10 kHz sidebands it is the other way round, but HIPWM has richer spectrum.

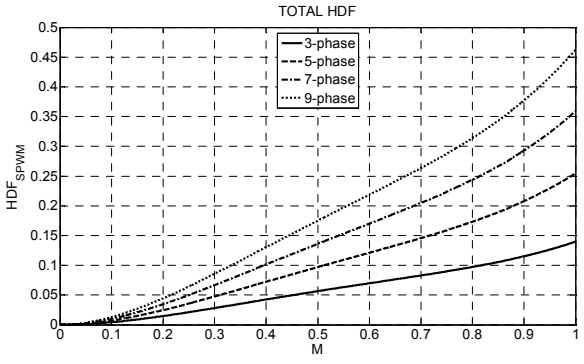

a)

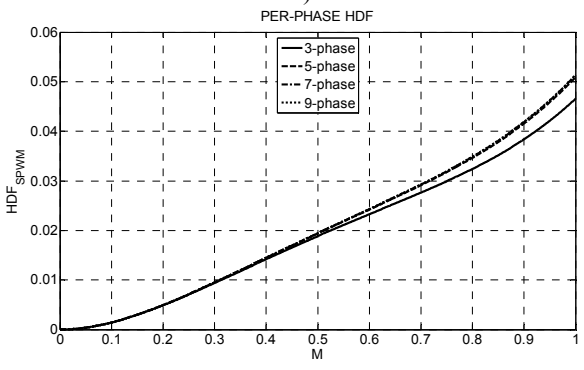

b)

Fig. 4. *SPWM HDF for phase numbers n = 3, 5, 7 and 9: a) total HDF and b) per-phase HDF.*

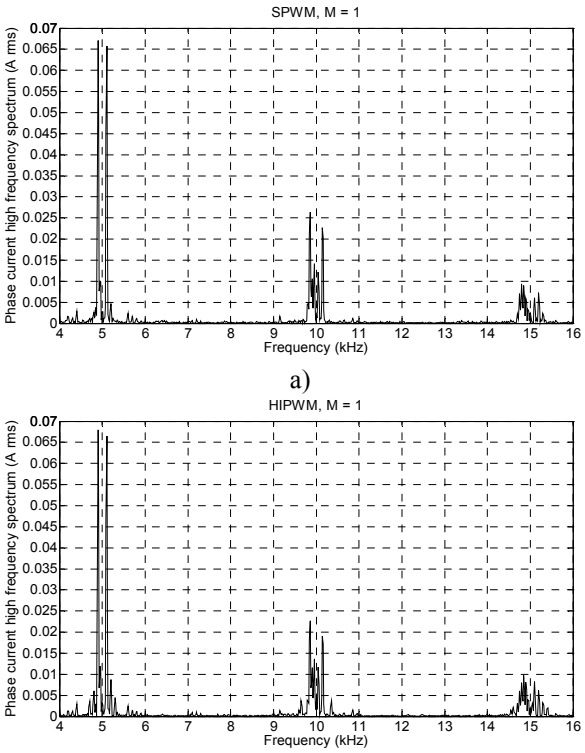

Fig. 5. *Experimentally recorded high frequency current spectrum for M=1 at 50 Hz for: a) SPWM and b) HIPWM.*

8. CONCLUSION

The paper presents an analytical analysis of harmonic losses (output current ripple rms) of multi-phase drives. Two approaches are elaborated, which can be used to obtain HDF for a PWM scheme of interest. It is shown that the total HDF of a multi-phase system is governed by the sum of individual polygon HDFs. Using individual polygon HDFs, it is possible to obtain corresponding *d-q* plane HDFs, without the need to use the much more complicated space vector approach.

The results obtained for the higher phase number topologies show very different characteristics when compared to a three-phase system, with regard to the application of harmonic injection PWM schemes and their influence on the harmonic losses. It is established that the reduction of the harmonic losses below the level offered by the SPWM is not possible in multi-phase systems, except in the three-phase one [1-6].

It is concluded that the total HDF can only be obtained if all the possible polygon connections of a multi-phase system are encompassed by the analysis. If precise evaluation of the impact of different harmonic groups, which map into different planes, is not of interest, then polygon HDFs are sufficient since per-phase HDF can be easily obtained from the total HDF, by dividing with the phase number. As the number of phases increases the total per-phase HDF for any CPWM tends to a constant value for any particular modulation index. Experimental results for SPWM and HIPWM, recorded on a five-phase induction motor drive, are included and these fully support theoretical considerations.

9. REFERENCES

[1] J.W. Kolar, H. Ertl, F.C. Zach, "Minimization of the harmonic RMS contents of the mains current of a PWM converter system based on the solution of an extreme value problem," *Proc. Int. Conf on Harmonics in Power Systems ICHPS,* Budapest, Hungary, 1990, pp. 234-243.

[2] J.W. Kolar, H. Ertl, F.C. Zach, "Analytically closed optimization of the modulation method of a PWM rectifier system with a high pulse rate," *Proc. Int. Power Conversion and Intelligent Motion Conf. PCIM,* Munich, Germany, 1990, pp. 209-223.

[3] H.W. Van der Broeck, H.C. Skudelny, "Analytical analysis of the harmonic effects of a PWM ac drive," *IEEE Trans. on Power Electronics*, vol. 3, no. 2, 1988, pp. 216-223.

[4] V. Blasko, "Analysis of a hybrid PWM based on modified space-vector and triangle-comparison methods," *IEEE Trans. on Industry Applications*, vol. 33, no. 3, 1997, pp. 756-764.

[5] A.M. Hava, R. Kerkman, T.A. Lipo, "Simple analytical and graphical methods for carrier-based PWM-VSI drives," *IEEE Trans. on Power Electronics*, vol. 14, no. 1, 1999, pp. 49-61.

[6] D.G. Holmes, T.A. Lipo, *Pulse Width Modulation for Power Converters - Principles and Practice,* IEEE Press, Piscataway, NJ, 2003.

[7] E. Levi, R. Bojoi, F.Profumo, H.A.Toliyat, S.Williamson, "Multiphase induction motor drives – A technology status review," *IET Electric Power Applications,* vol. 1, no. 4, 2007, pp. 489-516.

[8] P. Ferraris, M. Lazzari, "Phase numbers and their related effects on the characteristics of inverter fed induction motor drives," *Proc. IEEE Industry Applications Society Annual Meeting IAS*, Mexico City, Mexico, 1983, pp. 494-502.

[9] D. Dujic, M. Jones, E. Levi, "Analysis of output current ripple RMS in multi-phase drives using space vector approach," *IEEE Trans. on Power Electronics*, vol. 24, no. 8, 2009, pp. 1926-1938.

[10] D. Dujic, M. Jones, E. Levi, "Analysis of output current ripple RMS in multi-phase drives using polygon approach," *IEEE Trans. on Power Electronics*, (in press).

[11] S. Halasz, "PWM strategies of multi-phase inverters," *Proc. IEEE Industrial Electronic Society Annual Conf. IECON,* Orlando, FL, 2008, pp. 916-921.

[12] D. Dujic, M. Jones, E. Levi, "Continuous carrier based vs. space vector PWM for five phase VSI", *The Int. Conf. on "Computer as a tool" EUROCON,* Warsaw, Poland, 2007, pp. 1772-1779.

[13] A. Iqbal, E. Levi, M. Jones, S.N. Vukosavic, "Generalised sinusoidal PWM with harmonic injection for multi-phase VSIs," *Proc. IEEE Power Electronics Specialists Conf. PESC,* Jeju, Korea, 2006, pp. 2871-2877.

[14] E. Levi, D. Dujic, M. Jones, G. Grandi, "Analytical determination of DC-bus utilization limits in multi-phase VSI supplied AC drives", *IEEE Trans. on Energy Conversion*, vol. 23, no. 2, 2008, pp. 433-443.